

Causality-Inspired Safe Residual Correction for Multivariate Time Series

Jianxiang Xie¹ Yuncheng Hua¹ Mingyue Cheng² Flora Salim¹ Hao Xue^{3 1}

Abstract

While modern multivariate forecasters such as Transformers and GNNs achieve strong benchmark performance, they often suffer from *systematic errors* at specific variables or horizons and, critically, lack guarantees against performance degradation in deployment. Existing post-hoc residual correction methods attempt to fix these errors, but are inherently greedy: although they may improve average accuracy, they can also “help in the wrong way” by overcorrecting reliable predictions and causing local failures in unseen scenarios.

To address this critical “safety gap,” we propose CRC (*Causality-inspired Safe Residual Correction*), a plug-and-play framework explicitly designed to ensure *non-degradation*. CRC follows a divide-and-conquer philosophy: it employs a *causality-inspired encoder* to expose direction-aware structure by decoupling self- and cross-variable dynamics, and a *hybrid corrector* to model residual errors. Crucially, the correction process is governed by a strict *four-fold safety mechanism* that prevents harmful updates. Experiments across multiple datasets and forecasting backbones show that CRC consistently improves accuracy, while an **in-depth ablation study** confirms that its core safety mechanisms **ensure** exceptionally high non-degradation rates (NDR), making CRC a correction framework suited for safe and reliable deployment.

1. Introduction

Multivariate time series forecasting is a central component of decision-making in transportation, energy, finance,

and urban systems. Recent advances in deep forecasting—including attention-based models such as Informer (Zhou et al., 2021), FEDformer (Zhou et al., 2022), and Autoformer (Wu et al., 2021), 2D variation models such as TimesNet (Wu et al., 2022), channel-independent architectures such as PatchTST (Nie, 2022), and decomposition-based frameworks (Zeng et al., 2023)—have pushed benchmark performance to new heights. However, their “on-paper” average accuracy often masks a critical deployment challenge: these models can still fail *catastrophically* for specific horizons, sensors, or nodes (Makridakis et al., 2018; Lim & Zohren, 2021). In safety-critical or high-stakes applications, such horizon- or node-specific errors undermine reliability, robustness, and trustworthiness.

To mitigate these failures, the literature has long explored *residual correction* as a means to refine predictions. Classical approaches, including boosting (Freund & Schapire, 1997) and hybrid statistical–neural models (Zhang, 2003), treat residuals as exploitable structure. More recent post-hoc refinement models aim to enhance deep forecasting architectures by explicitly modeling residual patterns (Goel et al., 2017; Oreshkin et al., 2019; Wen et al., 2022). Unfortunately, these methods exhibit a fundamental weakness: they are *greedy*. By optimizing for average error reduction, they often “help in the wrong way”—overfitting to noisy residuals, distorting well-predicted points, and ultimately *degrading* performance where reliability matters most. This creates the **Corrector’s Dilemma**: how can a corrector capture *correctable systematic bias* without amplifying *uncorrectable random noise*?

In light of these limitations, we propose **Causality-inspired Safe Residual Correction (CRC)**, a plug-and-play framework designed from the ground up to *guarantee non-degradation*. Our central philosophy is that *safety cannot be an afterthought; it must be engineered into the correction process*. CRC resolves the Corrector’s Dilemma through a “defense-in-depth” architecture.

First, to isolate correctable systematic structure, we introduce a *causality-inspired encoder* that explicitly disentangles self- and cross-node dynamics. Motivated by causal directionality principles (Granger, 1969; Amblard & Michel, 2012), our encoder learns direction-sensitive interactions through dynamic gating, producing structured representa-

¹School of Computer Science and Engineering, University of New South Wales, Sydney, Australia ²State Key Laboratory of Cognitive Intelligence, School of Computer Science and Technology, University of Science and Technology of China, Hefei, China ³The Hong Kong University of Science and Technology (Guangzhou). Correspondence to: Hao Xue <haoxue@hkust-gz.edu.cn>.

tions that preserve directional influence and attenuate spurious correlations.

Second, we avoid reliance on a single “black-box” corrector. CRC adopts a *hybrid corrector* that decomposes the correction Δ into a conservative, interpretable *linear floor* based on Ridge Regression (Hoerl & Kennard, 1970) and a lightweight, expressive *nonlinear delta* modeled by an MLP. The linear component offers stability and interpretability, while the nonlinear component captures higher-order residual structure.

Most critically, the nonlinear “delta” is constrained by **four explicit safety mechanisms**: direction gating, quantile clipping, point-wise selection, and shrink-to-base blending. These mechanisms collectively serve as a *safety firewall* that prevents harmful corrections and ensures that no update is applied unless it is demonstrably safe, formalizing non-degradation at both point-wise and validation levels.

Contributions.

- **Causality-Aware Encoder.** A direction-sensitive encoder that separates self- and cross-node dynamics, providing structured per-node representations for systematic residual correction.
- **Hybrid Corrector with Explicit Safety.** A ridge ‘‘floor’’ plus a lightweight MLP delta”, governed by direction gating, quantile clipping, point-wise selection, and shrink-to-base blending.
- **Empirical Validation and Interpretability.** Comprehensive results across datasets and backbones demonstrate consistent accuracy improvements and exceptionally high non-degradation rates (NDR), with interpretability through directional priors and ridge coefficients.

2. Related Work

2.1. Forecasting and Residual Correction Models

Classical statistical models (e.g., ARIMA) provide strong biases but struggle with complex, high-dimensional data (Hyndman & Khandakar, 2008). Recent deep models, from RNNs (Hochreiter & Schmidhuber, 1997) to Transformers (Zhou et al., 2021) and decomposition architectures (Zeng et al., 2023; Wu et al., 2022), have achieved state-of-the-art accuracy on benchmarks. Independently, residual correction has a long history, from boosting (Freund & Schapire, 1997) to hybrid statistical-neural models (Zhang, 2003) and post-hoc refinement modules (Goel et al., 2017).

However, these two lines of work share a fundamental flaw: they are *greedy*. They are designed to optimize for *average* error (Wu et al., 2022; Goel et al., 2017). This focus

on average gain provides no mechanism to prevent, and often encourages, *harmful updates* that degrade performance on specific horizons or nodes. They are, by design, *unsafe*.

2.2. Safe and Causal Learning

A separate body of work has studied robustness from two main angles. **Safe Learning** aims to avoid harmful updates using tools like conformal prediction (Shafer & Vovk, 2008) (for intervals), selective prediction (Geifman & El-Yaniv, 2019) (for abstention), or robust objectives (Mohajerin Esfahani & Kuhn, 2017). **Causal Learning** aims to improve robustness under shifts by discovering and integrating causal structure (Granger, 1969; Runge et al., 2017; Schölkopf et al., 2021) into models, often via graph neural networks (Brouillard et al., 2020).

However, neither of these domains provides a complete solution for our goal. “Safe Learning” is *passive*; it focuses on uncertainty-aware abstention (Geifman & El-Yaniv, 2019; Shafer & Vovk, 2008) rather than *active correction*. “Causal Learning” is *descriptive*; it focuses on discovering a graph structure (Schölkopf et al., 2021; Brouillard et al., 2020) but does not, by itself, provide a framework for post-hoc correction that is guaranteed to be safe.

2.3. Our Contribution

In contrast to all prior work, CRC is the first framework designed not for *average* gain, but for *guaranteed* safety. It uniquely unifies three directions: (i) it leverages *causality-aware representations* to identify *what* to correct; (ii) it uses a *hybrid linear/nonlinear* corrector to model this correction; and (iii) it enforces *explicit safety mechanisms* to control *how* to correct without degradation.

3. Method

We present *Causality-aware Residual Correction* (CRC), a plug-and-play framework for *safe post-hoc forecasting correction*. Unlike conventional residual refinement methods that optimize average accuracy and may degrade reliable predictions, CRC is explicitly designed to *guarantee non-degradation* under deployment.

CRC takes as input a historical sequence $W \in \mathbb{R}^{B \times P \times N}$, where B is batch size, P the look-back window, and N the number of variables, together with a baseline forecast $\hat{Y}^{base} \in \mathbb{R}^{B \times H \times N}$ for horizon H . The corrected forecast is formulated as

$$\hat{Y} = \hat{Y}^{base} + \Delta, \quad (1)$$

where Δ is a structured and safety-constrained correction term. Our objective is *not* to maximize accuracy aggres-

sively, but to design Δ such that

$$\text{Error}(\hat{Y}) \leq \text{Error}(\hat{Y}^{base}), \quad (2)$$

thereby ensuring explicit non-degradation.

Overview. CRC follows a *safe-by-design* pipeline (Fig. 1) consisting of three stages: (1) exposing *correctable structure* in residuals via a causality-inspired encoder, (2) performing conservative hybrid correction within this structured space, and (3) enforcing a defense-in-depth safety firewall to prevent harmful updates.

3.1. Structured Residual Representation via a Causality-Inspired Encoder

Motivation. Directly correcting the raw residual $R = Y - \hat{Y}^{base}$ is unreliable, as it entangles *systematic, correctable bias* with *irreducible random noise*. Naive correctors that ignore this distinction often “help in the wrong way,” degrading already reliable predictions.

Key idea. Rather than performing causal discovery, we design a *causality-inspired encoder* whose role is to *expose direction-aware structure* that renders systematic residual components *recoverable* by downstream correction. This structured representation serves as an inductive bias for safe residual modeling.

Directional Encoding with Pairwise Interaction. Given a prior adjacency matrix $A \in \{0, 1\}^{N \times N}$ (where $A_{ij} = 1$ denotes a potential influence from j to i), the encoder separates self- and cross-node dynamics using a shared *pairwise interaction module* f_{pair} (Fig. 1, left), implemented via residual blocks (STCL-Core).

3.1.1. CAUSAL STATE ENCODING

Self-Dynamics. For each node i , the encoder first processes its own history to capture intrinsic temporal dynamics:

$$(R_i, \alpha_{i \rightarrow i}) = f_{\text{pair}}(W_{:, :, i}, W_{:, :, i}), \quad (3)$$

where $R_i \in \mathbb{R}^{B \times d}$ is a self-representation and $\alpha_{i \rightarrow i}$ is a self-gating coefficient.

Cross-Node Dynamics. For each potential source node j such that $A_{ij} = 1$, the same module processes the ordered pair (W_i, W_j) :

$$(R_j, \alpha_{j \rightarrow i}) = f_{\text{pair}}(W_{:, :, i}, W_{:, :, j}). \quad (4)$$

Internally, f_{pair} computes a 2×2 interaction matrix. The directed gate $\alpha_{j \rightarrow i}$ is *strictly extracted from the off-diagonal term* corresponding to $j \rightarrow i$ influence and passed through a tanh activation. This explicit isolation enables direction-sensitive representation without assuming causal identifiability.

Gated Aggregation. The final representation for node i is obtained via gated aggregation:

$$Z_i = \frac{1}{|\mathcal{N}(i)| + \alpha_{i \rightarrow i, \text{const}}} \left(\alpha_{i \rightarrow i} R_i + \sum_{j: A_{ij}=1} \alpha_{j \rightarrow i} R_j \right), \quad (5)$$

where normalization prevents high-degree nodes from dominating. This formulation yields a direction-aware embedding Z_i that exposes systematic residual structure relevant for correction.

3.1.2. MULTI-SCALE FEATURE PRIORS AND AUGMENTATION

To anchor residual correction in interpretable inductive biases, we augment the latent representation Z with a set of *multi-scale statistical feature priors* F (Fig. 1, Step 2). These priors summarize complementary temporal structures, including local distributional properties, short- and long-term dynamics, and coarse-grained frequency and correlation patterns. Rather than learning such properties implicitly, we expose them explicitly to improve correction stability under non-stationary conditions.

The resulting priors are aggregated through a row-normalized adjacency matrix A_{norm} to encode neighborhood context. The final structured input to correction is $Z_{\text{aug}} = [Z, F]$.

3.2. Safe Residual Correction with Explicit Guarantees

Challenge. Given structured features Z_{aug} , the core challenge is to correct systematic errors *without amplifying noise*. This is the *Corrector’s Dilemma*: expressive models improve average accuracy but risk catastrophic local degradation.

Strategy. CRC resolves this dilemma via a two-stage design: (i) a conservative hybrid corrector operating within a recoverable subspace, and (ii) a four-fold safety firewall that enforces non-degradation at both point-wise and validation levels.

3.2.1. HYBRID RESIDUAL CORRECTOR

CRC decomposes Δ into complementary components:

1. **Linear Floor** (Δ^{ridge}). For each node i , a ridge regressor maps $Z_{\text{aug}, i}$ to residuals $R_i = Y_i - \hat{Y}_i^{base}$:

$$W_i = \arg \min_W \|R_i - Z_{\text{aug}, i} W\|_2^2 + \lambda \|W\|_2^2, \\ \Delta_i^{\text{ridge}} = Z_{\text{aug}, i} W_i. \quad (6)$$

This closed-form projection stably recovers linearly explainable systematic bias.

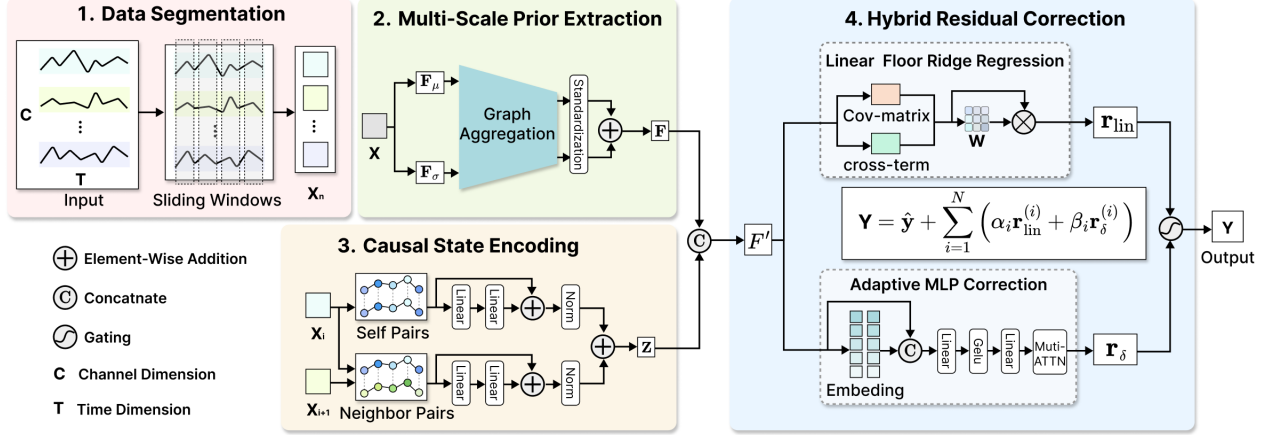


Figure 1. Overview of the Causality-aware Residual Correction (CRC) framework. CRC exposes structured residual representations via a causality-inspired encoder, applies hybrid linear–nonlinear correction, and enforces four explicit safety mechanisms to guarantee non-degradation.

2. **Nonlinear Delta (Δ^{MLP}).** A lightweight MLP captures remaining higher-order residual structure:

$$\Delta_i^{MLP} = f_\theta(Z_{aug,i}). \quad (7)$$

The unconstrained correction is $\Delta_i = \Delta_i^{ridge} + \Delta_i^{MLP}$.

3.2.2. FOUR-FOLD SAFETY FIREWALL

While expressive, Δ^{MLP} may overfit noise. CRC therefore enforces a defense-in-depth safety firewall:

- **Direction Gating.** Nonlinear updates are accepted only if aligned with the remaining residual direction, ensuring point-wise non-degradation.
- **Quantile Clipping.** Corrections are bounded by validation-based thresholds:

$$\Delta^{clip} = \text{clip}(\Delta, -\tau, \tau). \quad (8)$$

- **Point-wise Selection.** For each horizon and variable, the better of linear-only and hybrid correction is selected on validation data and frozen for deployment.
- **Shrink-to-Base Blending.** Blending weights (w_1, w_2) are activated only when validation improvement is statistically significant. Otherwise, the method reverts to the baseline forecast. The final safeguarded prediction is:

$$\hat{Y} = \hat{Y}^{base} + w_1 \Delta^{ridge} + w_2 \Delta^{clip}. \quad (9)$$

Formal non-degradation guarantees are provided in Appendix A.

3.2.3. SAFETY MECHANISM ANALYSIS: NECESSITY AND COMPLEMENTARITY

The four-fold safety firewall is not a collection of independent heuristics, but a deliberately structured defense-in-depth design. Each mechanism targets a distinct failure mode commonly observed in post-hoc residual correction. We briefly analyze these failure modes and explain why no single safeguard is sufficient.

Failure Mode I: Directional Misalignment. An expressive nonlinear corrector may propose updates with incorrect sign, especially under distribution shift or noisy residual estimates. Such updates increase point-wise error even when their magnitude is small. **Direction gating** directly addresses this issue by enforcing sign consistency between the nonlinear update and the remaining residual. This mechanism guarantees local non-degradation under MAE and MSE (Appendix A.1), but alone cannot prevent excessive correction magnitudes.

Failure Mode II: Scale Explosion. Even directionally correct updates may overshoot the true residual due to heavy-tailed noise or transient spikes. This leads to catastrophic degradation on a small subset of horizons or nodes. **Quantile clipping** mitigates this risk by bounding corrections using validation-calibrated thresholds, thereby controlling the worst-case update magnitude. However, clipping alone does not distinguish correctable systematic bias from irreducible noise.

Failure Mode III: Local Overfitting. A hybrid corrector may improve average validation error while degrading

performance on specific (i, h) pairs that were already well-predicted by the baseline. **Point-wise selection** explicitly prevents this by freezing, for each variable and horizon, the better of linear-only and hybrid corrections. This mechanism ensures that local degradation cannot be traded for global gain.

Failure Mode IV: Spurious Validation Gains. Small apparent improvements on validation data may arise from statistical fluctuation rather than genuine systematic structure. Deploying such fragile corrections leads to poor generalization. **Shrink-to-base blending** activates correction weights only when validation improvement exceeds a predefined margin, otherwise reverting to the baseline forecast. This final safeguard enforces a conservative deployment policy and stabilizes test-time performance.

Complementarity. These mechanisms operate at different levels: direction gating enforces *sign safety*, quantile clipping enforces *scale safety*, point-wise selection enforces *local safety*, and shrink-to-base blending enforces *validation-level safety*. Together, they form a necessary and sufficient safety firewall. Removing any single component exposes CRC to a corresponding failure mode, as empirically confirmed in the ablation study (Table 2).

3.3. Design Principles of Safe Residual Correction

CRC is shaped by a set of deliberately conservative design choices. Rather than maximizing expressiveness, our goal is to control when, where, and how residual correction is allowed to intervene. These principles emerged from repeated failure cases observed during development, where unconstrained correction improved average error but destabilized individual variables or horizons.

Separation of Recovery and Refinement. We explicitly separate residual correction into a linear recovery stage and a nonlinear refinement stage. In early experiments, we found that directly training a nonlinear corrector often caused it to relearn trivial residual patterns already captured by simple linear structure, leading to unnecessary variance. The ridge corrector therefore serves as a stable recovery floor, while the nonlinear module is restricted to modeling higher-order residual structure that cannot be recovered linearly.

Correct Only What Is Recoverable. CRC does not assume that residual errors are fully correctable. Instead, the causal encoder is used as a structural filter that highlights directional and temporal patterns likely to correspond to systematic bias. When such structure is weak or absent, correction is naturally suppressed. This prevents the model from expending capacity on transient noise or non-stationary fluctuations that do not generalize.

Safety Before Optimality. Throughout the design of CRC, we consistently favor bounded and reliable improvement over aggressive error minimization. We observed that even small, directionally incorrect updates could cause severe local degradation, despite improving average metrics. As a result, all nonlinear corrections are subjected to explicit safety constraints, and CRC is intentionally biased toward rejecting uncertain updates rather than risking degradation.

Validation-Calibrated Deployment. Validation performance is treated as a proxy for deployment risk, not as an additional optimization signal. Correction strength is activated only when improvement exceeds a conservative threshold estimated from validation data. When such evidence is insufficient, CRC deterministically reverts to the baseline forecast. This design choice prioritizes predictable behavior over marginal gains.

Additive and Interpretable Correction. All corrections in CRC are applied additively to the baseline forecast. This choice preserves the semantics of the base model and enables direct inspection of correction magnitude and direction. In practice, we found that additive updates are substantially easier to constrain and debug than multiplicative or recursive alternatives, particularly under distribution shift.

Taken together, these principles reflect a safety-first view of residual correction: corrections should be applied only when they are structurally justified, empirically supported, and unlikely to cause harm.

3.4. Complexity and Deployment

CRC is lightweight: ridge regression admits closed-form solutions, the MLP is small, and the encoder operates on fixed windows. Overall complexity is $O(BPN + N^2d)$, enabling efficient training and seamless integration with diverse forecasting backbones.

4. Experiments

4.1. Experimental Setup

Datasets and Baselines. We evaluate CRC on seven standard multivariate forecasting benchmarks: ETT (ETTh1, ETTh2, ETTm1, ETTm2), Weather, Electricity, and Traffic, under prediction horizons {96, 192, 336, 720}. CRC is applied as a plug-in corrector to four representative forecasting backbones: TimeXer, TimesNet, PatchTST, and DLinear. We report MSE and MAE (mean \pm std over three random seeds).

Evaluation Philosophy: Safety First. While average accuracy is important, our central hypothesis is that *post-hoc correction must be safe*. Accordingly, beyond MSE/MAE,

Dataset	Horizon	TimeXer		+ CRC		TimesNet		+ CRC		PatchTST		+ CRC		DLinear		+ CRC	
		MSE	MAE	MSE	MAE	MSE	MAE	MSE	MAE	MSE	MAE	MSE	MAE	MSE	MAE	MSE	MAE
ETTh1	96	0.3818	0.4029	0.3790	0.3989	0.3984	0.4163	0.3986	0.4152	0.3792	0.3988	0.3790	0.3898	0.3962	0.4108	0.3873	0.4099
	192	0.4285	0.4355	0.4100	0.4341	0.4373	0.4399	0.4473	0.4374	0.4240	0.4304	0.4218	0.4252	0.4450	0.4404	0.4392	0.4457
	336	0.4672	0.4494	0.4704	0.4533	0.4722	0.4584	0.4650	0.4696	0.4686	0.4578	0.4663	0.4751	0.4874	0.4654	0.4820	0.4701
	720	0.4988	0.4926	0.4967	0.5041	0.5181	0.4965	0.5140	0.5089	0.5193	0.5036	0.5260	0.5015	0.5126	0.5104	0.5242	0.5205
ETTh2	96	0.2854	0.3376	0.2858	0.3372	0.3423	0.3792	0.3373	0.3748	0.2924	0.3468	0.2906	0.3446	0.3414	0.3953	0.3172	0.3663
	192	0.3628	0.3892	0.3613	0.3885	0.4068	0.4117	0.4060	0.4118	0.3794	0.4044	0.3761	0.4007	0.4818	0.4792	0.4499	0.4504
	336	0.4109	0.4222	0.4132	0.4244	0.4398	0.4421	0.4382	0.4436	0.4183	0.4325	0.4116	0.4290	0.5929	0.5422	0.5773	0.5333
	720	0.4485	0.4534	0.4572	0.4661	0.4440	0.4564	0.4612	0.4644	0.4328	0.4532	0.4392	0.4567	0.8403	0.6611	0.8089	0.6381
ETTm1	96	0.3178	0.3563	0.3173	0.3544	0.3444	0.3806	0.3362	0.3770	0.3268	0.3667	0.3209	0.3617	0.3459	0.3737	0.3321	0.3664
	192	0.3616	0.3829	0.3620	0.3818	0.4222	0.4142	0.4051	0.4100	0.3718	0.3917	0.3694	0.3897	0.3818	0.3911	0.3704	0.3859
	336	0.3951	0.4067	0.3996	0.4085	0.4251	0.4276	0.4242	0.4269	0.3981	0.4080	0.3932	0.4050	0.4153	0.4150	0.4043	0.4125
	720	0.4524	0.4413	0.4616	0.4480	0.4879	0.4610	0.4911	0.4640	0.4586	0.4451	0.4618	0.4513	0.4730	0.4509	0.4672	0.4553
ETTm2	96	0.1706	0.2555	0.1701	0.2553	0.1858	0.2667	0.1842	0.2672	0.1868	0.2692	0.1849	0.2675	0.1934	0.2928	0.1836	0.2744
	192	0.2365	0.2987	0.2300	0.2961	0.2532	0.3100	0.2486	0.3095	0.2482	0.3070	0.2453	0.3046	0.2845	0.3614	0.2647	0.3364
	336	0.2954	0.3380	0.2874	0.3365	0.3237	0.3496	0.3240	0.3502	0.3109	0.3492	0.3069	0.3476	0.3849	0.4295	0.3479	0.3989
	720	0.3916	0.3935	0.3876	0.3921	0.4162	0.4050	0.4102	0.4035	0.4233	0.4157	0.4182	0.4123	0.5561	0.5235	0.5537	0.5137
Weather	96	0.1574	0.2047	0.1545	0.2018	0.1684	0.2185	0.1622	0.2120	0.1752	0.2174	0.1616	0.2071	0.1962	0.2561	0.1635	0.2158
	192	0.2041	0.2475	0.2008	0.2450	0.2345	0.2735	0.2069	0.2538	0.2214	0.2562	0.2043	0.2465	0.2389	0.2992	0.2086	0.2631
	336	0.2610	0.2899	0.2530	0.2852	0.2902	0.3095	0.2682	0.2965	0.2801	0.2975	0.2531	0.2847	0.2811	0.3306	0.2543	0.3004
	720	0.3400	0.3406	0.3189	0.3283	0.3593	0.3539	0.3230	0.3360	0.3560	0.3475	0.3257	0.3319	0.3454	0.3819	0.3277	0.3540
Electricity	96	0.1406	0.2426	0.1345	0.2326	0.1676	0.2702	0.1564	0.2591	0.1802	0.2734	0.1509	0.2481	0.2102	0.3014	0.1516	0.2517
	192	0.1572	0.2558	0.1517	0.2485	0.1897	0.2914	0.1762	0.2787	0.1875	0.2797	0.1639	0.2586	0.1938	0.2799	0.1722	0.2649
	336	0.1759	0.2754	0.1682	0.2666	0.1981	0.2988	0.1898	0.2916	0.2042	0.2959	0.1800	0.2762	0.2230	0.3191	0.1833	0.2836
	720	0.2161	0.3091	0.1990	0.2957	0.2313	0.3249	0.2232	0.3213	0.2435	0.3281	0.2142	0.3060	0.2440	0.3323	0.2132	0.3099
Traffic	96	0.4277	0.2715	0.4221	0.2641	0.5913	0.3160	0.5571	0.2972	0.4583	0.2985	0.4298	0.2808	0.6965	0.4287	0.4889	0.3084
	192	0.4587	0.2761	0.4558	0.2698	0.6120	0.3278	0.5847	0.3059	0.4804	0.3104	0.4543	0.2919	0.6014	0.3747	0.4839	0.3083
	336	0.4762	0.2925	0.4699	0.2847	0.6543	0.3484	0.6192	0.3183	0.4963	0.3174	0.4698	0.2990	0.6077	0.3769	0.5036	0.3187
	720	0.5195	0.3101	0.5135	0.3031	0.6711	0.3490	0.6546	0.3339	0.5308	0.3341	0.5044	0.3174	0.6482	0.3982	0.5404	0.3383

Table 1. Results on ETTh1, ETTh2, ETTm1, ETTm2, Weather, Electricity, and Traffic datasets (horizons 96/192/336/720). Lower is better. Bold indicates that CRC outperforms the corresponding baseline for that metric.

Model / Experiment	MSE ↓	NDR ↑
Baseline (DLinear on Elec.)	0.198	N/A
Full CRC Model (Ours)	0.173	95.0
<i>Group 1: Ablating the Hybrid Corrector</i>		
1a. "MLP-Only" (No Ridge Floor)	0.181	70.0
1b. "Ridge-Only" (No MLP Delta)	0.192	94.0
<i>Group 2: Ablating the Safety Firewall</i>		
2a. No Quantile Clipping	0.176	85.0
2b. No Direction Gating	0.175	88.0
2c. No Point-wise Selection	0.174	90.0
2d. No Shrink-to-Base Blending	0.174	82.0
<i>Group 3: Ablating the Causal Encoder</i>		
3a. "No-Graph" (Self-Only)	0.185	93.0
3b. "No-Encoder" (Simple Features)	0.195	90.0

we introduce and emphasize the **Non-Degradation Rate (NDR)**, defined as the fraction of (node, horizon) pairs for which the corrected forecast is *no worse than* the baseline. An NDR of 100% indicates perfect safety and deployment-readiness.

Implementation Details. CRC is implemented in PyTorch and trained on NVIDIA GPUs (e.g., A100). Training proceeds in two stages: (i) MTL pre-training of the encoder, and (ii) training of the hybrid residual corrector. We use AdamW (encoder) and Adam (MLP) optimizers with learning rate 1×10^{-4} and batch size 32. The encoder and corrector are trained for up to 80 and 60 epochs, respectively, with early stopping based on validation MAE. The adjacency matrix is constructed using correlation-based K -NN graphing with $K = 5$. Quantile clipping uses $Q = 0.80$, and shrink-to-base blending threshold is $\varepsilon = 0.01$.

4.2. Main Results: Safety First, Accuracy as a By-product

4.2.1. CORE SAFETY GUARANTEE: NON-DEGRADATION RATE (NDR)

The defining property of CRC is its explicit non-degradation guarantee. As shown in Table 2, the **full CRC model** achieves a remarkably high NDR of **95.0%**, demonstrating that the proposed four-fold safety firewall effectively resolves the *Corrector's Dilemma*. In contrast, removing any safety component leads to a substantial drop in NDR, confirming that CRC's reliability is the result of deliberate

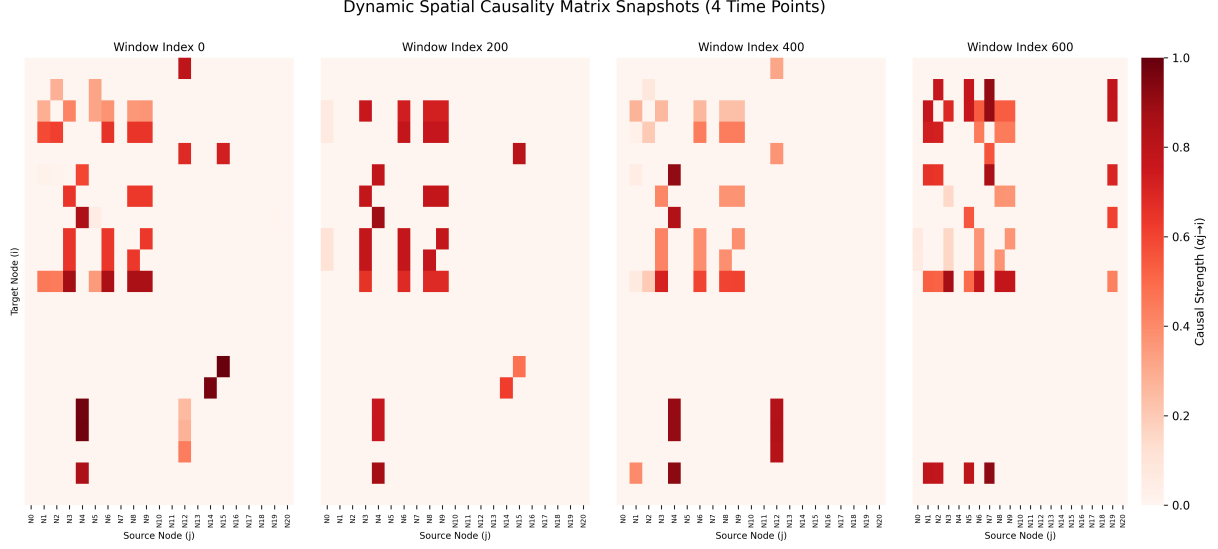


Figure 2. Dynamic Spatial Causality Snapshots ($N = 4$). Time-evolution of learned directional influence strengths $S_t[i, j]$ ($j \rightarrow i$) by CRC (TimesNet backbone) on the Weather dataset. The encoder captures strongly non-stationary and context-dependent dependencies across four representative windows ($\Delta t = 200$).

design rather than chance. These results establish CRC as a deployment-ready correction framework.

4.2.2. ACCURACY IMPROVEMENTS UNDER SAFETY CONSTRAINTS

Under the above safety guarantees, CRC consistently improves forecasting accuracy. As shown in **Table 1**, CRC yields overall MSE/MAE reductions across all seven datasets and four backbones. Improvements are most pronounced in **long-horizon** and **structurally complex** scenarios, where systematic biases accumulate and naive correction is most risky.

For example, on the **Traffic** dataset at $H = 336$, CRC substantially reduces the DLinear baseline’s MSE from **0.6077** to **0.5036**, demonstrating its effectiveness in complex, highly coupled real-world systems. On more challenging datasets such as **ETTm1**, where residual structures are weaker and closer to noise, CRC yields more modest average improvements. Importantly, the proposed safety firewall suppresses aggressive corrections in such regimes, thereby preventing performance degradation while preserving stability.

4.3. Comparison with Instance-Aware Revision (PIR)

We compare CRC with the recent post-forecasting identification and revision (PIR) framework (Liu et al., 2025), which focuses on instance-level failure retrieval and revision, but does not incorporate explicit safety control mechanisms. Table 3 reports relative performance differences $\Delta = \text{PIR} - \text{CRC}$, where positive values indicate that CRC

achieves lower error.

Several observations can be made. First, PIR can achieve competitive or even slightly better performance in some short-horizon settings, indicating that aggressive instance-level revision can be effective when errors are localized. However, these gains are not consistent across datasets, backbones, or forecasting horizons. Second, CRC exhibits more stable advantages in long-horizon forecasting and on structurally complex datasets, such as **Traffic**, **Electricity**, and **Weather**, where post-hoc corrections are more prone to error accumulation. Finally and most importantly, PIR lacks mechanisms to explicitly prevent harmful updates, whereas CRC enforces safety constraints through its hybrid correction and safety firewall design. As a result, CRC maintains a consistently high non-degradation rate (NDR), making it a more reliable and robust choice for safety-critical forecasting scenarios.

4.4. Ablation Study: Validating CRC’s Design Principles

We conduct an extensive ablation study (Table 2) on DLinear–Electricity to examine the contribution of each component in CRC.

Causality-Inspired Encoder. Removing the encoder (Group 3) leads to noticeably weaker performance compared to the full model (MSE increases from 0.173 to 0.195), indicating that structured, direction-aware representations provide an important performance benefit for effective residual correction.

Dataset	Horizon	TimeXer		TimesNet		PatchTST		DLinear	
		Δ MSE	Δ MAE						
ETTh1	96	-0.0030	-0.0019	-0.0076	-0.0002	-0.0033	0.0012	-0.0143	-0.0159
	192	-0.0060	-0.0041	0.0057	0.0086	0.0072	0.0038	-0.0152	-0.0227
	336	-0.0264	-0.0213	0.0150	0.0104	0.0077	-0.0011	-0.0100	-0.0211
	720	-0.0537	-0.0391	-0.0130	-0.0019	-0.0260	-0.0245	-0.0472	-0.0485
ETTh2	96	0.0092	0.0048	0.0097	0.0012	0.0134	0.0064	-0.0312	-0.0313
	192	0.0057	0.0045	0.0160	0.0072	0.0059	0.0013	-0.0819	-0.0634
	336	0.0038	0.0016	0.0118	0.0024	0.0464	0.0210	-0.1643	-0.1093
	720	-0.0492	-0.0311	-0.0162	-0.0114	-0.0092	-0.0067	-0.3919	-0.2011
ETTm1	96	0.0017	0.0016	0.0278	0.0050	0.0031	-0.0007	-0.0161	-0.0134
	192	0.0070	0.0042	-0.0251	-0.0130	-0.0004	-0.0017	-0.0034	-0.0049
	336	0.0244	0.0155	0.0198	0.0101	0.0108	0.0080	-0.0053	-0.0065
	720	0.0134	0.0100	0.0239	0.0100	0.0032	0.0017	-0.0012	-0.0133
ETTm2	96	0.0089	0.0057	0.0018	0.0018	0.0101	0.0075	-0.0056	-0.0104
	192	0.0100	0.0079	0.0234	0.0095	0.0097	0.0134	-0.0217	-0.0304
	336	0.0196	0.0065	0.0170	0.0088	0.0081	0.0034	-0.0399	-0.0529
	720	0.0434	0.0249	0.0128	0.0095	0.0128	0.0107	-0.1477	-0.1087
Weather	96	0.0025	0.0032	0.0058	0.0060	0.0104	0.0069	0.0185	0.0112
	192	0.0052	0.0040	0.0141	0.0072	0.0147	0.0105	0.0194	-0.0001
	336	0.0110	0.0078	0.0148	0.0085	0.0249	0.0133	0.0287	0.0016
	720	0.0281	0.0197	0.0420	0.0250	0.0983	0.0461	0.0403	0.0030
Electricity	96	0.0125	0.0084	0.0016	0.0019	0.0151	0.0009	0.0174	-0.0017
	192	0.0083	0.0045	0.0038	0.0003	0.0121	0.0014	0.0068	-0.0039
	336	0.0058	0.0034	-0.0018	-0.0046	0.0120	-0.0012	0.0127	-0.0056
	720	0.0000	-0.0007	-0.0042	-0.0053	0.0098	-0.0010	0.0248	0.0041
Traffic	96	0.0139	0.0059	-0.0441	0.0068	0.0202	0.0022	0.0201	0.0016
	192	0.0072	0.0082	-0.0447	0.0081	0.0127	-0.0049	0.0241	0.0057
	336	0.0101	0.0003	-0.0622	0.0127	0.0142	-0.0060	0.0224	-0.0047
	720	0.0185	0.0019	-0.0566	0.0071	0.0096	-0.0064	0.0236	-0.0073

Table 3. Relative performance of PIR (Post-forecasting Identification and Revision) vs CRC ($\Delta = \text{PIR} - \text{CRC}$). Negative = PIR better, positive = CRC better.

Hybrid Corrector and Safety Firewall. Using an unconstrained MLP corrector (Group 1a) yields severe degradation, with NDR dropping sharply to 70.0%, while a linear-only corrector remains safe but underpowered. Removing any component of the safety firewall (Group 2) results in substantial NDR loss, confirming that CRC’s safety properties arise from a defense-in-depth design.

Together, these results highlight a progressive design principle in CRC: *structured representations facilitate recoverable residuals, hybrid correction balances flexibility and stability, and explicit safety mechanisms are essential for preventing degradation.*

4.5. Interpretability: Dynamic Structural Validation

This analysis does not aim to validate causal discovery, but to examine whether the encoder captures meaningful, time-varying directional structure that supports safe correction. Figure 2 visualizes the evolution of the instantaneous spatial influence matrix S_t .

The learned structure exhibits strong non-stationarity. Overall interaction strength varies significantly across windows, key directional paths emerge and decay over time, and event-driven influence bursts (e.g., toward node N16) appear transiently. These observations confirm that the encoder adapts to changing contexts, providing the hybrid corrector with timely and relevant structural priors for non-stationary residual correction.

5. Conclusion

In this work, we introduced Causality-aware Residual Correction (CRC), a plug-and-play framework designed to safely and effectively correct systematic errors from baseline multivariate forecasters. Our approach addresses two key challenges: the lack of directional awareness in standard models and the risk of performance degradation in post-hoc correction. CRC pairs a causality-inspired encoder, which learns dynamic, directed interactions by separating self- and cross-node dynamics, with a hybrid corrector that stabilizes a non-linear MLP delta upon a robust linear ridge “floor”. Most critically, our four-fold safety mechanism ensures high non-degradation rates (NDR), as **validated by our diagnostic experiments (Table 2)**, making it a reliable tool for real-world deployment. Empirical results confirmed that CRC consistently improves accuracy across diverse backbones and datasets (Table 1) while providing valuable interpretability.

Despite these promising results, our work has several limitations. First, the “causality-aware” encoder is *inspired* by causal principles but is not a causal discovery method. Its effectiveness relies on a pre-defined adjacency matrix A , which is currently derived from simple correlation. The quality of this prior graph can influence the representations, and a poorly specified graph may limit the corrector’s ability to isolate true directional dynamics. Second, our safety mechanisms, while crucial for achieving high NDR, are inherently conservative. The quantile clipping and shrink-to-base blending may prevent the model from correcting very large, yet correctable, baseline errors, potentially sacrificing maximum accuracy for robustness.

Future work can proceed in several exciting directions. To address the reliance on a static prior, CRC could be integrated with online or constraint-based causal discovery algorithms. This would allow the graph A to be learned from data or even co-optimized with the correction task. Furthermore, we plan to explore more adaptive safety mechanisms, such as replacing the static quantile τ with dynamic, uncertainty-based bounds (e.g., from conformal prediction), to achieve an even better trade-off between safety and performance.

References

- Amblard, P.-O. and Michel, O. J. The relation between granger causality and directed information theory: A review. *Entropy*, 15(1):113–143, 2012.
- Brouillard, P., Lachapelle, S., Lacoste, A., Lacoste-Julien, S., and Drouin, A. Differentiable causal discovery from interventional data. *Advances in Neural Information Processing Systems*, 33:21865–21877, 2020.

Freund, Y. and Schapire, R. E. A decision-theoretic generalization of on-line learning and an application to boosting. *Journal of computer and system sciences*, 55(1):119–139, 1997.

Geifman, Y. and El-Yaniv, R. Selectivenet: A deep neural network with an integrated reject option. In *International conference on machine learning*, pp. 2151–2159. PMLR, 2019.

Goel, H., Melnyk, I., and Banerjee, A. R2n2: Residual recurrent neural networks for multivariate time series forecasting. *arXiv preprint arXiv:1709.03159*, 2017.

Granger, C. W. Investigating causal relations by econometric models and cross-spectral methods. *Econometrica: journal of the Econometric Society*, pp. 424–438, 1969.

Hochreiter, S. and Schmidhuber, J. Long short-term memory. *Neural computation*, 9(8):1735–1780, 1997.

Hoerl, A. E. and Kennard, R. W. Ridge regression: Biased estimation for nonorthogonal problems. *Technometrics*, 12(1):55–67, 1970.

Hyndman, R. J. and Khandakar, Y. Automatic time series forecasting: the forecast package for r. *Journal of statistical software*, 27:1–22, 2008.

Lim, B. and Zohren, S. Time-series forecasting with deep learning: a survey. *Philosophical transactions of the royal society a: mathematical, physical and engineering sciences*, 379(2194), 2021.

Liu, Z., Cheng, M., Zhao, G., Yang, J., Liu, Q., and Chen, E. Improving time series forecasting via instance-aware post-hoc revision. *arXiv preprint arXiv:2505.23583*, 2025.

Makridakis, S., Spiliotis, E., and Assimakopoulos, V. The m4 competition: Results, findings, conclusion and way forward. *International Journal of forecasting*, 34(4):802–808, 2018.

Mohajerin Esfahani, P. and Kuhn, D. Data-driven distributionally robust optimization using the wasserstein metric. 2017.

Nie, Y. A time series is worth 64words: Long-term forecasting with transformers. *arXiv preprint arXiv:2211.14730*, 2022.

Orshkin, B. N., Carpow, D., Chapados, N., and Bengio, Y. N-beats: Neural basis expansion analysis for interpretable time series forecasting. arxiv 2019. *arXiv preprint arXiv:1905.10437*, 2019.

Runge, J., Nowack, P., Kretschmer, M., Flaxman, S., and Sejdinovic, D. Detecting causal associations in large nonlinear time series datasets. *arXiv preprint arXiv:1702.07007*, 2017.

Schölkopf, B., Locatello, F., Bauer, S., Ke, N. R., Kalchbrenner, N., Goyal, A., and Bengio, Y. Toward causal representation learning. *Proceedings of the IEEE*, 109(5):612–634, 2021.

Shafer, G. and Vovk, V. A tutorial on conformal prediction. *Journal of Machine Learning Research*, 9(3), 2008.

Wen, Q., Zhou, T., Zhang, C., Chen, W., Ma, Z., Yan, J., and Sun, L. Transformers in time series: A survey. *arXiv preprint arXiv:2202.07125*, 2022.

Wu, H., Xu, J., Wang, J., and Long, M. Autoformer: Decomposition transformers with auto-correlation for long-term series forecasting. *Advances in neural information processing systems*, 34:22419–22430, 2021.

Wu, H., Hu, T., Liu, Y., Zhou, H., Wang, J., and Long, M. Timesnet: Temporal 2d-variation modeling for general time series analysis. *arXiv preprint arXiv:2210.02186*, 2022.

Zeng, A., Chen, M., Zhang, L., and Xu, Q. Are transformers effective for time series forecasting? In *Proceedings of the AAAI conference on artificial intelligence*, volume 37, pp. 11121–11128, 2023.

Zhang, G. P. Time series forecasting using a hybrid arima and neural network model. *Neurocomputing*, 50:159–175, 2003.

Zhou, H., Zhang, S., Peng, J., Zhang, S., Li, J., Xiong, H., and Zhang, W. Informer: Beyond efficient transformer for long sequence time-series forecasting. In *Proceedings of the AAAI conference on artificial intelligence*, volume 35, pp. 11106–11115, 2021.

Zhou, T., Ma, Z., Wen, Q., Wang, X., Sun, L., and Jin, R. Fedformer: Frequency enhanced decomposed transformer for long-term series forecasting. In *International conference on machine learning*, pp. 27268–27286. PMLR, 2022.

A. Theoretical Analysis and Proofs

This appendix presents formal guarantees for the proposed CRC framework. We first show pointwise and validation-level non-degradation, then give a probably approximately non-degrading (PAND) bound on the test set. Finally, we explain why the causal-inspired encoder facilitates the recoverability of systematic residuals.

A.1. A. Safe Residual Correction Guarantees

Let Y denote the ground-truth future, $\widehat{Y}_{\text{base}}$ the baseline forecast, Δ_{lin} the linear (ridge) correction, and define the residual after the linear floor by

$$e = Y - (\widehat{Y}_{\text{base}} + \Delta_{\text{lin}}).$$

Let δ be the nonlinear increment and $\delta' = \text{clip}(\delta, -\tau, \tau)$ the clipped update with a validation-quantile threshold $\tau > 0$.

Assumption A.1 (Directional gating and clipping). The nonlinear update satisfies either $\text{sign}(\delta) = \text{sign}(e)$ or $|\delta| \leq \frac{1}{2}\tau$, and the deployed update is $\delta' = \text{clip}(\delta, -\tau, \tau)$.

Proposition A.2 (Pointwise non-degradation under MAE). *Under Assumption A.1, if $0 \leq |\delta'| \leq \min\{|e|, \tau\}$, then*

$$|e - \delta'| \leq |e|.$$

An analogous inequality holds for MSE when $\text{sign}(\delta') = \text{sign}(e)$ and $|\delta'| \leq |e|$.

Proof. When $\text{sign}(\delta') = \text{sign}(e)$ and $|\delta'| \leq |e|$, we have $|e - \delta'| = ||e| - |\delta'|| \leq |e|$. If $|\delta| \leq \frac{1}{2}\tau$ and $|\delta'| \leq \tau \leq |e|$, the same inequality holds. \square

Proposition A.3 (Validation-level non-degradation). *On the validation set, use pointwise selection between (1) linear-only and (2) linear+clipped updates, and apply shrink-to-base blending: activate blending only when the validation improvement is at least $\varepsilon \geq 0$. Then the validation error satisfies*

$$\mathcal{L}_{\text{val}}(\text{CRC}) \leq \mathcal{L}_{\text{val}}(\text{lin}).$$

Consequently, $\text{NDR}_{\text{val}} = 100\%$ (or $\geq 100\% - \xi$ when a positive ε disables tiny gains).

Let m be the number of validation points and define Bernoulli indicators $Z_k = \mathbb{1}\{|e_k^{\text{test}}(\text{CRC})| \leq |e_k^{\text{test}}(\text{base})|\}$ for test non-degradation at each point k .

Theorem A.4 (Probably approximately non-degrading (PAND)). *Assume i.i.d. sampling between validation and test. With probability at least $1 - \delta$,*

$$\overline{Z}_{\text{test}} \geq \overline{Z}_{\text{val}} - \sqrt{\frac{\log(1/\delta)}{2m}},$$

where \overline{Z} is the empirical mean of $\{Z_k\}$. Hence

$$\text{NDR}_{\text{test}} \geq 1 - \xi - \sqrt{\frac{\log(1/\delta)}{2m}} \quad \text{with probability at least } 1 - \delta.$$

Sketch. Apply Hoeffding's inequality to the Bernoulli indicators Z_k and use that $\mathbb{E}[Z_k^{\text{test}}] = \mathbb{E}[Z_k^{\text{val}}]$ under the i.i.d. assumption. \square

Proposition A.5 (Risk upper bound with blending threshold). *Assume pointwise MAE is bounded in $[0, M]$. If blending is enabled only when the validation improvement is at least $\varepsilon > 0$, then*

$$\mathcal{L}_{\text{test}}(\text{CRC}) \leq \mathcal{L}_{\text{test}}(\text{base}) - \varepsilon + \tilde{O}\left(\sqrt{1/m}\right),$$

where the $\tilde{O}(\cdot)$ term collects the validation–test generalization gaps bounded via Hoeffding's inequality.

A.2. B. Why the Causal-Inspired Encoder Helps

Consider the following data-generating mechanism for node i :

$$Y_{:,i} = f_i(W_{:,i}) + \sum_{j \in \text{Pa}(i)} g_{j \rightarrow i}(W_{:,j}) + \varepsilon_i, \quad (10)$$

where the baseline $\hat{Y}_{\text{base},i}$ already captures $f_i(\cdot)$ but may miss the cross-node systematic term $\sum_{j \in \text{Pa}(i)} g_{j \rightarrow i}(\cdot)$. Let the encoder output be

$$Z_i = \alpha_{i \rightarrow i} R_i + \sum_{j \in \mathcal{N}(i)} \alpha_{j \rightarrow i} R_j,$$

with directional weights $\alpha_{j \rightarrow i}$ and neighborhood $\mathcal{N}(i)$ that covers $\text{Pa}(i)$.

Proposition A.6 (Linear recoverability via ridge projection). *Suppose each $g_{j \rightarrow i}$ is first-order linearizable as $g_{j \rightarrow i}(W_{:,j}) \approx \phi_j^\top \psi(W_{:,j})$, and Z_i forms a bounded-distortion linear embedding of $\{\psi(W_{:,j})\}_{j \in \mathcal{N}(i)}$. Then the ridge solution*

$$W_i^* = \arg \min_W \|R_i - Z_i W\|_2^2 + \lambda \|W\|_2^2$$

yields $\Delta_{\text{ridge},i} = Z_i W_i^*$, the minimum-norm projection of $\sum_{j \in \text{Pa}(i)} g_{j \rightarrow i}(W_{:,j})$ onto $\text{span}(Z_i)$, and its approximation error is controlled by the embedding distortion and the ridge term λ .

Intuition. Directional gating promotes $\alpha_{j \rightarrow i} > 0$ for potential parent nodes, so $\text{span}(Z_i)$ covers the true systematic residual space. Ridge regression then gives the orthogonal projection that optimally trades bias and variance. \square

Remark A.7 (Practical implications). The encoder provides direction-aware inductive bias rather than causal discovery: it amplifies the recoverable systematic components for the ridge floor, while the nonlinear head offers conservative refinements guarded by directional gating, quantile clipping, pointwise selection, and shrink-to-base blending.